

# Passive Hybrid MEMS for High-Temperature Telemetric Measurements

Daniele Marioli, *Member, IEEE*, Emilio Sardini, *Member, IEEE*, and Mauro Serpelloni

**Abstract**—A contactless sensor represents an attractive solution for high-temperature measurements in harsh environments, where the use of cables is not suitable, and where the temperature values are beyond those permitted by active electronic circuits. Temperature sensors have a wide variety of applications in automated processes for temperature control and regulation. This paper describes a passive sensing device suitable for high-temperature measurements consisting of a microfabricated temperature-sensitive variable capacitor and a planar inductor designed for high-temperature environments. Another readout inductor constitutes, together with the planar inductor, a telemetric system, which is a coupled transformer with the readout connected to the measurement electronics. The proposed passive hybrid microelectromechanical systems (MEMS) consists of an interdigitated capacitor bonded to the planar inductor. The hybrid sensor behaves as an  $LC$  resonant circuit in which the interdigitated capacitor represents the capacitance and the planar inductor is the inductance. The temperature induces a displacement of the conductive electrodes of the interdigitated capacitor toward the fixed electrodes realizing a temperature-sensitive variable capacitor. An equivalent circuit scheme of the variable capacitor and the planar inductor has been analyzed. Two telemetric measurement methods, relying on a frequency variation output, have been tested. The whole system has been tested in the laboratory, and several results are reported. Finally, the sensor prototype was fabricated and successfully characterized up to 330 °C as a proof of concept of temperature sensing through passive wireless communication. The proposed telemetric temperature system can be a solution for efficiency monitoring and predictive maintenance for harsh and complex environments, thereby eliminating the need for physical contacts, active elements, or power supplies, which cannot withstand harsh environments.

**Index Terms**—Autonomous sensor, contactless telemetric system, high-temperature measurement, microelectromechanical systems (MEMS), wireless system.

## I. INTRODUCTION

HIGH-TEMPERATURE measurements are required in several industrial applications, such as process control, safety evaluation, reliability prediction, product liability, and quality control. Some harsh environments are high-temperature rooms, industrial ovens, and rooms dedicated to experiments involving ionizing radiation. Moreover, in several applications, there is the necessity to maintain a hermetic environment, such

as in controlled drying processes and pressurized fluids. In these cases, the environment is unsuitable for commercial electronic circuits that do not work in the presence of temperatures greater than 100 °C; thus, the measurement system is often divided into two subsystems, one of which is the sensitive element constituted by a passive probe, such as a resistance temperature detector, thermocouple, or optical fiber [1]. The sensing element is positioned in the harsh environment, whereas the second part of the measurement system, consisting of all the active devices of the conditioning electronics required to extract the measurement information, is outside in a safe zone. In fact, the readout part works at lower temperatures, which are compatible with the specific requirements of the active devices. Usually, the two subsystems are connected by wires or optical fibers, requiring a direct link between the safe and harsh zones. In some cases, the harsh environment is hermetic as well, for security purposes or functioning requirements, and in this case, a direct hardware connection between the probe and the conditioning electronics is not possible. Optical instruments such as pyrometers or infrared optical sensors sometimes offer a solution. In [2], an infrared temperature measurement system able to measure temperatures between 500 °C and 1300 °C is described. Many applications of contactless temperature measurements are made with radiometric surface thermometers commonly referred to as infrared thermometers for a lower range of values. In [3], a high-temperature probe station is designed to characterize active and passive devices and circuits at temperatures ranging from room temperature to above 500 °C. In [4], the authors propose the use of microwave radiometry to noninvasively measure and control the temperature during the microwave sintering processes. In [5], the magnetic coupling between sensor and transducer constitutes the contactless measurement; the temperature sensor is the NiFe alloy that is strongly temperature dependant. The experiments were carried out in a range from room temperature up to 90 °C. In [6], a temperature sensor based on an interferometer and suitable for use in a pulse power system is reported. This sensor has a range of 20 °C to 350 °C.

A telemetric system represents an interesting solution for connecting the probe positioned in the hazardous zone with the conditioning electronics in the safe zone. Moreover, they represent a viable solution when the measurement environment is contained in an enclosed and hermetic space, and the required wire link through the separating wall, between the harsh and safe zones, is not possible due to the presence of high pressure or the use of expensive connecting techniques. In the literature, telemetric systems are applied in industrial fields, for example, when the measuring environment is not accessible,

Manuscript received June 30, 2009; revised September 28, 2009. First published December 31, 2009; current version published April 7, 2010. The Associate Editor coordinating the review process for this paper was T. Lipe.

The authors are with the Department of Electronics for Automation, University of Brescia, 25123 Brescia, Italy (e-mail: emilio.sardini@ing.unibs.it; mauro.serpelloni@ing.unibs.it).

Color versions of one or more of the figures in this paper are available online at <http://ieeexplore.ieee.org>.

Digital Object Identifier 10.1109/TIM.2009.2038026

since it is inside a hermetic environment [7]–[9]. In [7], the telemetric system is used to monitor the pressure inside a high-temperature environment. The sensing technique is based on a change of the resonant frequency of an  $LC$  circuit, depending on the sensor capacitance. Because of their small size and stable characterization, these  $LC$  sensors are particularly suitable for transmitting high energy for short distances, as required in harsh medical and industrial environments, for instance, high-temperature pressure sensors [10], high-temperature chemical sensors [11], and humidity sensors [12]. Other examples of a passive telemetric system for chemical monitoring are quoted in [13] and [14]. In [15], a passive wireless temperature sensor operating in a harsh environment for high-temperature rotating component monitoring is reported. The novel high- $k$  temperature-sensitive ceramic material has been developed to work up to 235 °C. The temperature sensor consists of a ceramic multilayer capacitor integrated with a planar inductor, which forms an  $LC$  resonant circuit.

In [16], a novel telemetric system is presented for high-temperature measurements in harsh industrial environments. A novel microfabricated temperature-sensitive variable capacitor connected to a planar inductor, which is realized in a thick-film technology, constitutes the sensitive element. The common working principle of the microelectromechanical systems (MEMS) is based on the structural deformation that appears as a consequence of a temperature increase. Temperature sensors of various designs, microfabrication techniques, and testing procedures have been presented in the literature [17], [18]. The proposed variable capacitor consists of a cascade of bent beam structures to enhance the sensitivity of the sensor [19].

In this paper, a hybrid MEMS characterization is reported. The equivalent circuit scheme of the variable capacitor and the planar inductor has been analyzed. The characterization is done for temperature up to 330 °C. The frequency behavior is reported and verified with experimental data. The telemetric communication is characterized as well. To telemetrically acquire the temperature value, two different measurement techniques are reported. The techniques are based on impedance measurements, to identify a particular resonant frequency, or a frequency point that has a particular property such as a minimum of the phase, or to compensate the distance changes through the measurement of three resonance frequencies. To experimentally verify the characteristics of the proposed measurement system, a telemetric apparatus consisting of a hybrid sensor and a readout inductor has been tested in a temperature-controlled measurement oven. The reported experimental results have been measured with the aid of an impedance analyzer.

## II. DESCRIPTION AND CHARACTERIZATION OF THE HYBRID MEMS

The proposed telemetric system is schematically shown in Fig. 1: on the left, the hybrid MEMS is placed into the harsh environment, whereas on the right, the conditioning electronics are in the safe zone. A wall separates the two zones, and the two subsystems communicate through a magnetic field. This wall has no magnetic or conductive properties so that guarantees the magnetic coupling. In industrial ovens, a thin separation wall

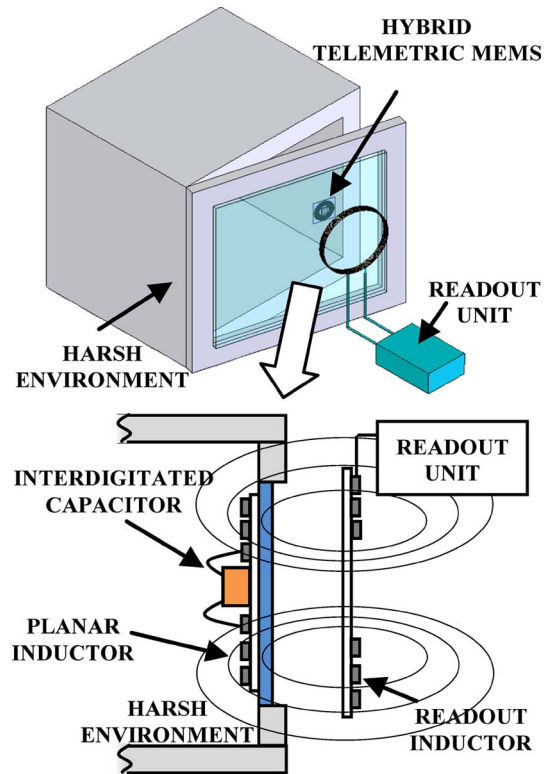


Fig. 1. Block diagram of the telemetric system.

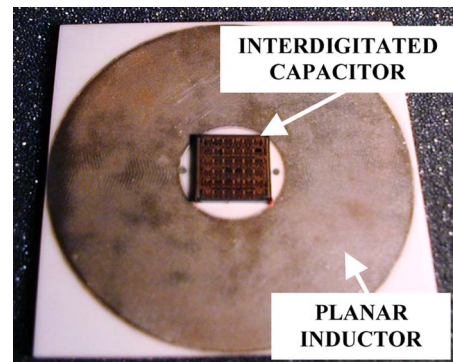


Fig. 2. Image of the hybrid telemetric MEMS.

made of tempered glass is used for visual inspection of the internal process. The small area and the thermal and physical settings of these glasses guarantee low heat dispersion; thus, the temperature inside the oven is uniform with the temperature near the wall.

In Fig. 2, the proposed hybrid MEMS placed inside the harsh environment consists of the microfabricated temperature-sensitive variable capacitor developed using the MetalMUMPs process [19] and the planar inductor with high-temperature characteristics. The MetalMUMPs process uses a six-mask process with eight thin film layers. The DIE is positioned centrally to the inductor and bonded to it. Therefore, with respect to other technologies, like SOIMUMPs, PolyMUMPs, etc., which could have resulted in comparable capacitances, the nickel of the MetalMUMPs process exhibits higher coefficient of thermal expansion, being approximately  $13 \times 10^{-6}$  /K. The hybrid telemetric MEMS behaves as an  $LC$  resonant circuit

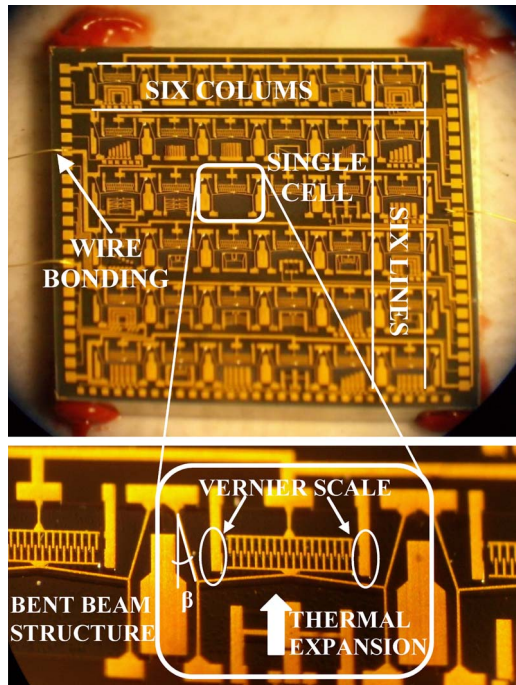


Fig. 3. Microscope image of DIE.

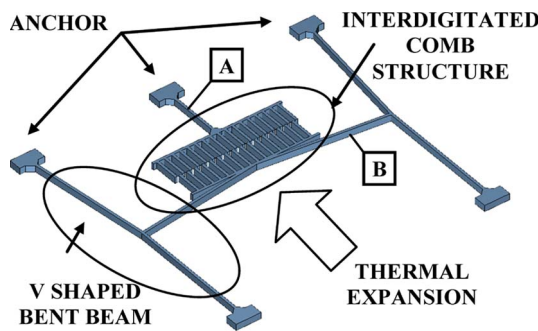


Fig. 4. Image of a bent beam structure.

in which an interdigitated capacitor represents the capacitance, and the planar inductor is the inductance.

*A. Microfabricated Temperature-Sensitive Variable Capacitor*

The layout of the variable capacitor (Fig. 3) is organized into 36 cells having capacitive behavior and connected in parallel. The single cell is based on a cascade of bent beam structures. Two Vernier scales were laterally positioned to optically evaluate the deformations. The device is built directly over a silicon nitride isolation layer with a 1- $\mu\text{m}$  air gap or over a 25- $\mu\text{m}$ -deep trench, which is etched into the substrate [19]. The maximum operating temperature is limited by the maximum operating limit of nickel (350 °C).

In Fig. 4, a simulation model is reported: the single structure consists of a V-shaped beam anchored at two ends. The temperature variation induces a thermal expansion of the structure, generating a displacement of the central apex, which is connected to an interdigitated comb. The prototypes have been made relatively big, since the minimum line width and space for the nickel structural layer is 8  $\mu\text{m}$ . The prototype has a beam

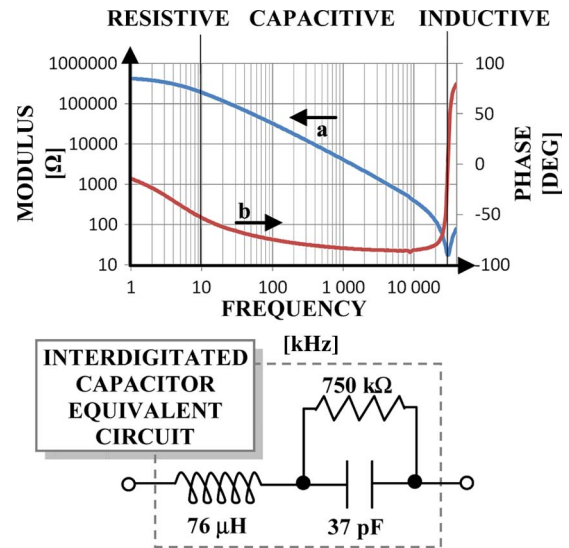


Fig. 5. Equivalent model of the interdigitated capacitor and an impedance diagram measured at 270 °C [(a) modulus and (b) phase].

length of 500  $\mu\text{m}$  and a width of 10  $\mu\text{m}$  with a vertex of 7°. During the design of the hybrid MEMS, some analyses of the mechanical resonant frequencies of the structure have been done. The single cell of the microfabricated variable capacitor has the two parts labeled as A and B, as shown in Fig. 4. Comsol finite-element methods have been used to determine the mechanical behaviors of the structure. The two parts have mechanical resonant frequencies of about A = 25 kHz and B = 15 kHz, respectively, at the first mode of vibration.

The DIE was placed inside a controlled oven, and using a wired connection, it was characterized with temperature by the impedance analyzer (HP4194A). In Fig. 5, the impedance diagram of the interdigitated capacitor obtained at 270 °C is reported. As can be seen, a resistive behavior due to the dielectric losses is shown at lower frequencies, whereas at higher frequencies, a resonant frequency is visible due to the parasitic inductance. For a large frequency interval, from 10 kHz up to 10 MHz, the variable capacitor mainly behaves as a capacitance. An equivalent circuit of the variable capacitor is also presented, and the approximate values of the parasitic inductance (76  $\mu\text{H}$ ), resistance (750 k $\Omega$ ), and capacitance (37 pF) are shown.

The DIE has been connected to an alumina substrate and bonded to two different pads for the signal connections. An impedance analyzer has been used to electrically characterize the device. In Fig. 6, the impedance module diagrams of the variable capacitor measured at different temperatures are reported. The temperature has been changed from about 100 °C to 330 °C. Three different zones have been identified: 1) In the lower frequencies, an increase in the parasitic resistance in parallel to the capacitance causes a change from the capacitive to the resistive behavior. 2) In the middle frequency, the increasing of the capacitance can be observed. 3) Whereas in the highest frequencies, as the temperature increases, the resonant frequency decreases. It can be noticed that the parallel resistance is temperature dependent: it decreases if temperature increases, and its behavior is prevalent in the low-frequency range. Above

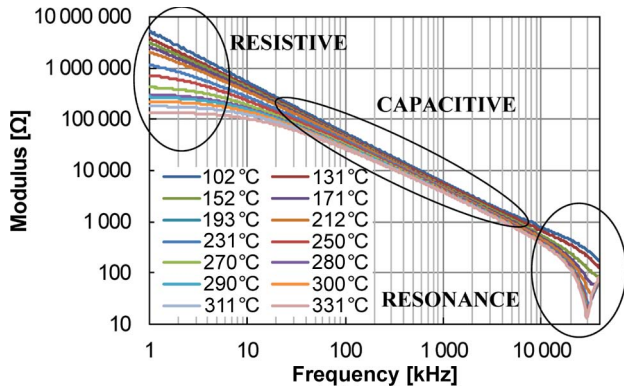


Fig. 6. Impedance module of the interdigitated capacitor measured at different temperatures.

TABLE I  
CHARACTERISTICS OF THE PLANAR INDUCTORS

| Inductors | Technology   | Windings | Length $S$ [ $\mu\text{m}$ ] | Length $T$ [ $\mu\text{m}$ ] |
|-----------|--------------|----------|------------------------------|------------------------------|
| A1        | Thick films  | 120      | 75                           | 89                           |
| A2        | Thick films  | 120      | 75                           | 89                           |
| B1        | Photolithog. | 75       | 170                          | 130                          |
| B2        | Photolithog. | 110      | 110                          | 90                           |

10 MHz, a resonance effect due to the parasitic inductance tends to be more visible; this is due to the capacitance increase as a function of temperature. Experimental results show that the variable capacitor mainly behaves as a capacitor between 0.1 and 10 MHz.

### B. Planar Inductors

Several inductors have been fabricated by exploiting two different technologies. To read out the temperature information, it is necessary to design and fabricate an appropriate inductor having a specific inductance value and a good quality factor at high temperatures. Formulas for the inductance value estimation of circular spiral inductors only give approximate results, and the use of electromagnetic simulation helped to find the desired characteristics. In Table I, the characteristics of the fabricated inductors are reported. The planar inductors A1 and A2 are obtained using thick-film technology by screen printing and microcutting by a laser. During the screen printing, two conductive (QM14 commercialized by Du Pont) films, one overlapping the other, were deposited to reach a thickness of about 20  $\mu\text{m}$  over an alumina substrate (50 mm  $\times$  50 mm  $\times$  0.63 mm). The conductive film has a resistivity of about 1.5–2.5 m $\Omega$ /sq. The deposited film was dried for 10–15 min at 150  $^{\circ}\text{C}$  and then was fired in a conveyor furnace for 30 min with a peak temperature of 850  $^{\circ}\text{C}$ . The microcutting process consists of material ablation by a laser. The inductors have the external diameter of 50 mm, 120 windings each of about 89- $\mu\text{m}$  width, and spaced 75  $\mu\text{m}$  from the others (Fig. 7).

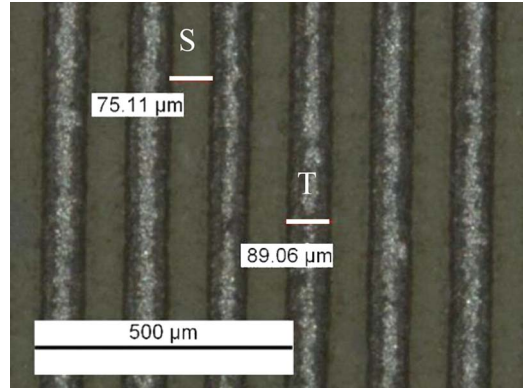


Fig. 7. Microscope image of the inductor A1 realized by thick-film deposition on alumina.

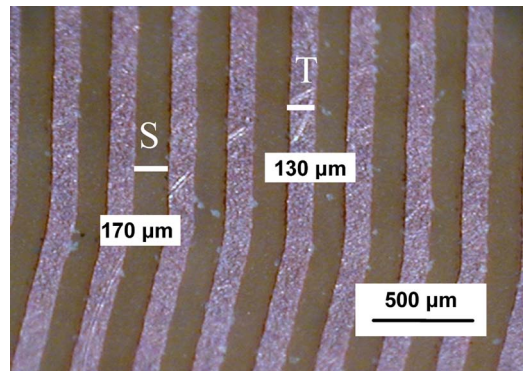


Fig. 8. Microscope image of the inductor B1 realized by photolithography.

A second set of planar inductors was realized by photolithographic technology on a substrate that can operate at high temperature. The 85N polyimide laminate is commercialized by Arlon and has a good resistance to high temperature (up to 280  $^{\circ}\text{C}$ ). The substrate is a double-layer laminate with copper (35  $\mu\text{m}$ ). The photolithographic process uses light to transfer the spiral pattern from a photomask to a light-sensitive chemical (photoresist) on the substrate (Fig. 8). A series of chemical treatments then engrave the exposure pattern into the material underneath the photoresist.

The planar inductors were realized with different patterns, as reported in Table I. The thick-film technology and the microcutting process permit the fabrication of inductors with a higher winding density. The number of windings is smaller in the photolithographic process so as to obtain a similar surface occupied.

In Fig. 9, the equivalent model of the planar inductor is reported: the inductance is in series with the resistance and the capacitance, modeling the wire connections and the capacitive behavior, respectively. In Fig. 9 as well, the module diagrams of the impedance of the inductor A1 are reported: the impedance is monitored for a wide temperature interval from 23  $^{\circ}\text{C}$  up to 340  $^{\circ}\text{C}$ . A resistive behavior is shown at lower frequencies, and it is dependent on temperature since the resistivity of the conductive paste increases with temperature, whereas at higher frequencies, a resonant frequency is visible due to the parasitic capacitance resonating with the inductor. For a large frequency

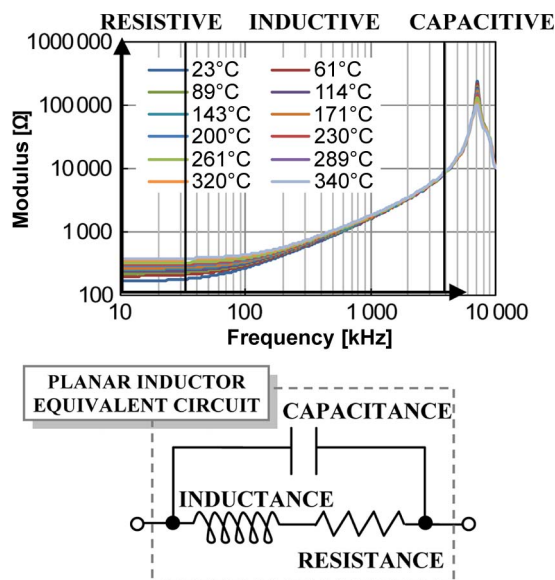


Fig. 9. Equivalent model of the planar inductor and impedance diagrams at different temperatures.

TABLE II  
EQUIVALENT CIRCUIT PARAMETERS OF THE INDUCTORS

| Inductors | Inductance (μH) | Capacitance (pF) | Resistance (Ω) |
|-----------|-----------------|------------------|----------------|
| A1        | 256             | 1.95             | 169            |
| A2        | 255             | 1.92             | 174            |
| B1        | 68              | 1.8              | 50             |
| B2        | 138             | 1.1              | 96             |
| Readout   | 14.5            | 91.4             | 20             |

interval, i.e., from 100 kHz to 7 MHz, the planar inductor has quite pure inductive behavior. A temperature variation does not induce a variation of the inductance and capacitance parameters, whereas there is an increasing of the resistance as expected. The equivalent circuit parameters of every single inductor (consisting of inductance and resistance in series both in parallel with a capacitance) were measured by the impedance analyzer (HP4194A), and their values are reported in Table II.

### C. Hybrid MEMS

The DIE is fixed to the planar inductor by a high-temperature ceramic adhesive (Resbond 931C) commercialized by Cotronics. The contact pads are bonded to the inductor terminals. The mass of the hybrid MEMS is about 8 g: 6 g (alumina), 0.2 g (DIE), and the remaining mass is due to the glue. The hybrid telemetric MEMS were characterized at room temperature. The impedance characterization of the hybrid sensor was obtained by changing the temperature from about 50 °C to 330 °C with steps of 10/20 °C. The impedance analyzer (HP4194A) was set to measure module, phase, and equivalent circuit parameters (inductance, capacitance, and resistance) of the device under

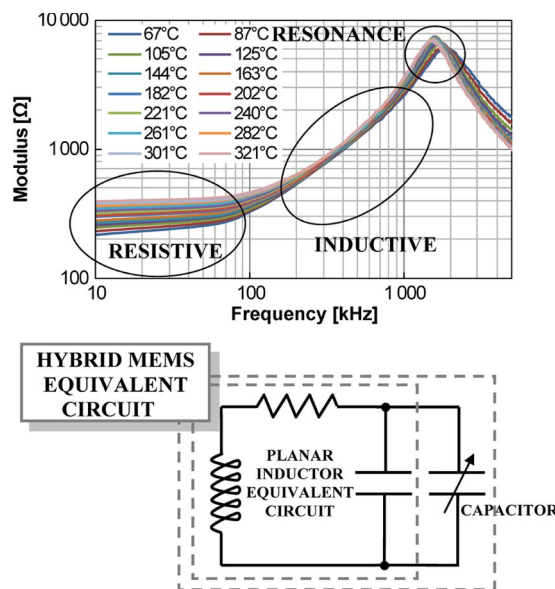


Fig. 10. Impedance module of the hybrid MEMS measured at different temperatures.

TABLE III  
EQUIVALENT CIRCUIT PARAMETERS OF THE HYBRID SENSORS

| Hybrid sensors | Inductance (μH) | Capacitance (pF) | Resistance (Ω) |
|----------------|-----------------|------------------|----------------|
| Hybrid A1      | 255             | 22.1             | 172            |
| Hybrid B1      | 67              | 22               | 51             |

test for every temperature step. The impedance module diagrams measured for different frequencies and temperatures are reported in Fig. 10. Three different zones have been identified: in the lower frequencies, an increase in the parasitic resistance due to increasing temperature can be noticed. In the middle frequency, an inductive behavior can be observed. At high frequencies, the resonant frequency decreases with temperature rise, as expected. The resistance, inductance, and capacitance, i.e.,  $R_S$ ,  $C_S$ , and  $L_S$ , respectively, of the hybrid MEMS were measured with an impedance analyzer (HP4194A), and the results are reported in Table III. The hybrid sensor realized by the thick-film inductor A1 shows wider temperature range and lower resonant frequency but higher resistance than the inductor B1. A high-temperature range permits a wide range of applications, whereas a lower resistance permits to improve the quality factor of the resonance. The experimental data reported in the following sections were obtained by the hybrid sensor A1. For applications with temperatures up to 280 °C, the hybrid sensor B1 could be used as well, improving the quality factor of the resonances. The equivalent circuit of the hybrid MEMS is reported in Fig. 10. The capacitance is increased by a value of about 2 pF due to the parasitic capacitance of the inductor, which is a slight increase since the capacitance (evaluated at room temperature) of the variable capacitor is about 20 pF. Since the capacitance and inductance of the planar inductor are stable when temperature changes, no influence on the sensitivity of the hybrid MEMS is introduced.

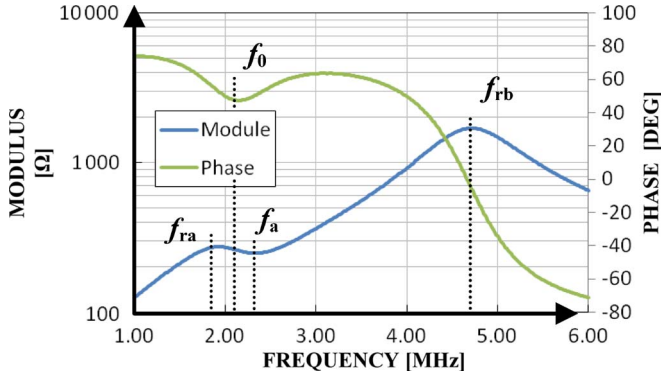


Fig. 11. Modulus and phase of the impedance measured from the terminals of the readout inductor.

#### D. Telemetric Model and Measurement Techniques

An inductor, named readout inductor, is placed close to the hybrid MEMS: the two inductors constitute a telemetric coupled system. Moreover, the readout inductor is directly connected to an impedance analyzer (HP4194A). The readout inductor is a planar spiral fabricated in thick-film technology, and it has 30 windings, each of 250- $\mu\text{m}$  width and spaced 250  $\mu\text{m}$  from the others. The external diameter is 50 mm wide. For characterization purposes of the telemetric system, the impedance is measured by the impedance analyzer (HP4194A) at 25  $^{\circ}\text{C}$  at a distance of between a few centimeters, as seen from the terminals of the readout inductor. Fig. 11 shows the measured modulus and phase of the impedance: three resonant frequencies ( $f_{ra}$ ,  $f_{rb}$ , and  $f_a$ ) can be observed on the modulus curve, whereas another significant point ( $f_o$ ) corresponding to the minimum of phase in the interval between  $f_{ra}$  and  $f_a$  is highlighted.

In the literature, two different measurement techniques suitable to obtain the capacitance for a telemetric system are reported and are known as 1) 3-Resonances [20] and 2) Min-Phase methods [7]. Both are based on the impedance measurements at the readout inductor: the 3-Resonances method requires the measurement of  $f_{ra}$ ,  $f_{rb}$ , and  $f_a$  and allows compensation of the relative distance change of the two inductors, whereas the Min-Phase only measures  $f_o$ , but the distance between the two inductors should be fixed. In [20], three resonance frequencies are measured with the aim to calculate the sensor capacitance and to compensate the distance variations (3-Resonances method). According to [20], the capacitive value of the variable capacitor is obtained as the product of a constant term  $\alpha$  and one calculated by the measures of  $f_{ra}$ ,  $f_{rb}$ , and  $f_a$ , i.e.,

$$C'_S = \alpha \frac{(2\pi f_{ra})^2 + (2\pi f_{rb})^2 - (2\pi f_a)^2}{(2\pi f_a)^2} \quad (1)$$

$$\alpha = \frac{L_1 C_R}{L_2}. \quad (2)$$

The constant term  $\alpha$  can automatically be obtained by calibration or calculated by measuring the parameters of the equivalent circuit of the readout inductor and the hybrid sensor, where  $L_1$  and  $L_2$  represent the inductance values of the readout and hybrid MEMS, and  $C_R$  is the parasitic capacitance of the readout inductor. The equivalent circuit parameters, consisting

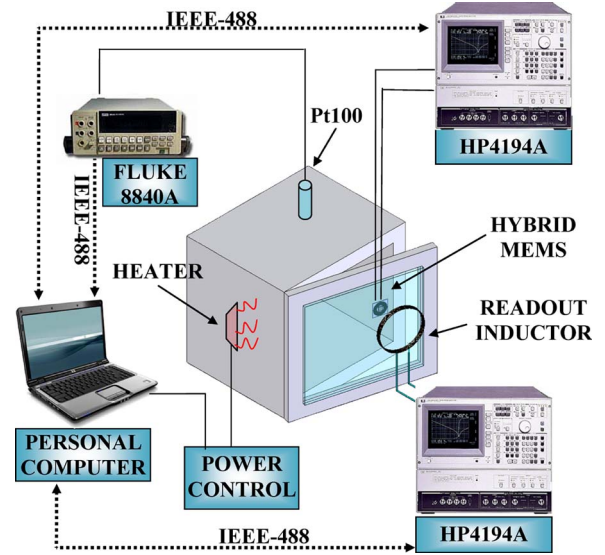


Fig. 12. Block diagram of the experimental setup.

of the series of an inductance and a resistance both in parallel with a capacitance, were measured by the impedance analyzer (HP4194A), and its values are  $L_1$  of about 14.5  $\mu\text{H}$  and  $C_R$  of about 91.4 pF. The equivalent circuit parameters of the hybrid sensor are reported in Table III.

The Min-Phase method also measures the impedance of the terminals of the readout inductor; thus, the capacitive value of the sensor is related to the frequency at which the phase, in a short frequency interval, is at its minimum value; this frequency approximately corresponds to

$$f_o = \frac{1}{2\pi\sqrt{C_S L_S}} \quad (3)$$

where  $C_S$  and  $L_S$  are the inductance and capacitance of a simplified equivalent circuit of the hybrid MEMS seen as a resonant  $LC$  circuit.

### III. EXPERIMENTAL SETUP

An experimental setup has been designed to test the telemetric measurement system at high temperatures. In Fig. 12, a block diagram of the experimental setup is shown.

The measurement chamber is made of two walls: 1) the internal wall of aluminum and 2) the external wall of steel; between them, a thermoresistive wool (Superwool607 commercialized by Thermal Ceramics) is interposed. The total thickness of the measurement chamber is about 3 cm, and the maximum space of the chamber is 30 cm  $\times$  30 cm  $\times$  13 cm. In one side, a window for visual inspection of the internal process was realized by a temperate glass with a maximum working temperature of about 500  $^{\circ}\text{C}$ . The window is a square of 12  $\times$  12 cm. Inside the chamber, an IR heater of 500 W was mounted, permitting a controlled temperature of over 350  $^{\circ}\text{C}$ . Three thermoresistances (Pt100) measure the internal temperature in three different points; each one is connected to a multimeter (Fluke 8840A). The three values are used to assure that the temperature is uniformly distributed. During the execution of the test, the thermoresistance difference of about 0.2  $\Omega$  that corresponds to less than 1  $^{\circ}\text{C}$  was observed.

A personal computer, running a developed LabVIEW virtual instrument, is connected to the multimeters through an IEEE 488 bus and to the input of the power control through the digital output of the input–output board. The PC monitors the temperature inside the oven and controls the IR heater by turning on and off the power circuit. The PC also controls the impedance analyzer storing and analyzing the data. The hybrid sensors were tested in the oven. Initially, one hybrid sensor was directly connected to an impedance analyzer (HP4194A) for a direct measurement of the sensor capacitance, and then another hybrid sensor was used for telemetric measurements. The measurement of the resonant frequency can be influenced by the capacitive variation due to the possible oscillation of the mechanical structure. It may happen that if a structure is externally mechanically driven, then it begins to oscillate at its mechanical resonant frequency. As previously reported, the two structures oscillate at 15 and 25 kHz at the first mode of vibration, whereas the electrical resonances are higher, i.e., on the order of megahertz. Furthermore, the selective filter of the impedance analyzer is a bandpass filter with a bandwidth of less than 1 kHz, which filters out any modulation effects on electrical resonance caused by mechanical oscillations. Any effect of capacitively driving mechanical resonances in the capacitor structure can be neglected. Externally, the readout inductor was connected to the input terminal of an impedance analyzer (HP4194A). In Fig. 8, the temperatures of the three thermoresistances were monitored during a thermal cycle of heating and cooling. The diagram shows inertia in the heating process that is fast at low temperatures and slow at high temperatures. The cooling process is obtained by heat dispersion, stabilizing the temperature by the IR heater.

IV. EXPERIMENTAL RESULTS

As previously reported, the impedance analyzer HP4194A is connected to the readout inductor to evaluate the telemetric system behavior and directly connected to the hybrid sensor to measure, as reference, the impedance of the sensor. The readout inductor was axially positioned to the hybrid sensor at about 1 cm to the hybrid sensor inside the chamber, whereas outside the readout, it was connected to the impedance analyzer. In fact, the two different methods, as previously reported, use impedance diagrams to calculate the sensor capacitance. In Fig. 13, modulus (a) and phase (b) diagrams of the impedance for several temperatures are reported. The diagrams are reported for a range of frequencies in which the resonant frequencies  $f_{ra}$  and  $f_a$  are visible. As expected, an increase in temperature generates a decrease of the values of the resonant frequencies.

In Fig. 14, the values of the sensor capacitance obtained by the direct measurements of the impedance are compared for different temperatures with the values calculated by the impedance diagrams using the Min-Phase and the 3-Resonances techniques. The values calculated are close to the reference directly measured with the impedance analyzer. Fig. 14 shows a quasilinear behavior of the sensor. The linear polynomial interpolations are also reported in Fig. 14. The results reported in Fig. 14 show a sensitivity of about 60 fF/°C.

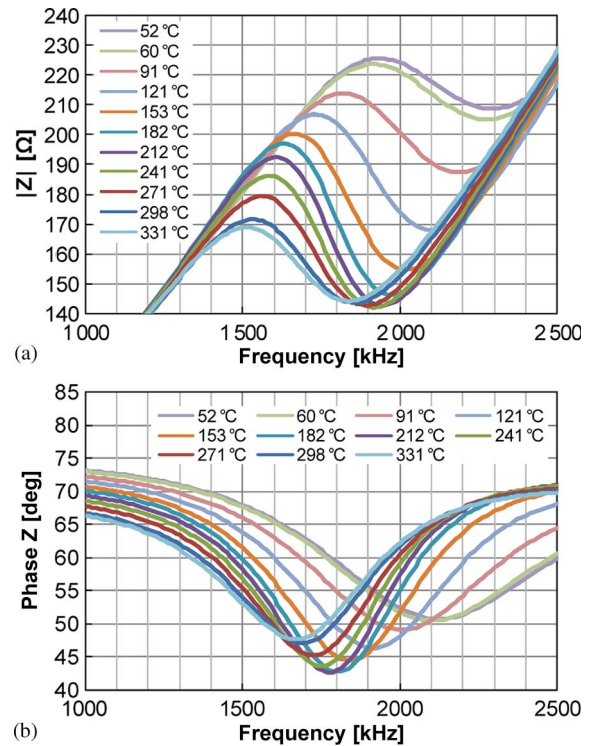


Fig. 13. (a) Modulus and (b) phase of the hybrid MEMS measured with the impedance analyzer at different temperatures.

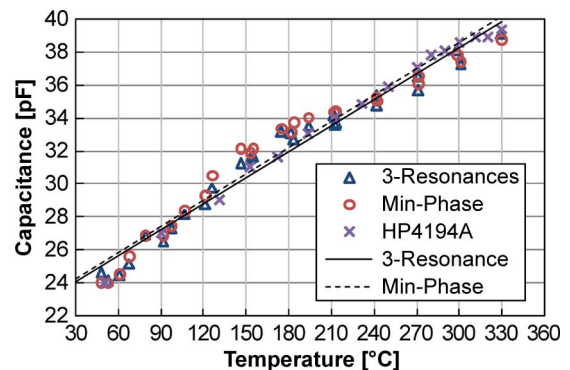


Fig. 14. Capacitance sensor values directly measured and compared with the Min-Phase and 3-Resonances calculated values.

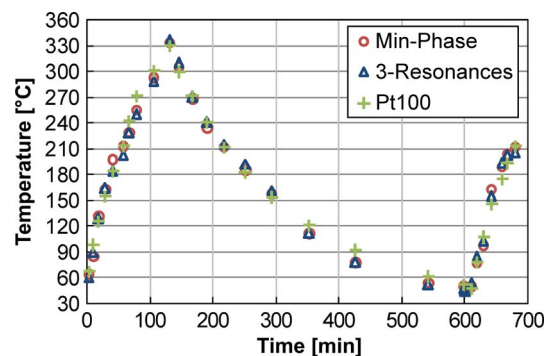


Fig. 15. Temperature values measured with the reference sensor (Pt100) are compared with the values calculated by the Min-Phase and 3-Resonances methods.

In Fig. 15, the temperatures measured with the reference sensor (Pt100) are compared with the values calculated by the Min-Phase and 3-Resonances methods. The temperature

values are obtained using the polynomial interpolation diagrams reported in Fig. 14. Fig. 15 shows a good agreement of the temperature values during both the heating and the cooling process. The hybrid MEMS follows the trend of the temperature signal that it has estimated to about  $1.9\text{ }^{\circ}\text{C}/\text{min}$  and  $0.6\text{ }^{\circ}\text{C}/\text{min}$  during the heating and cooling process, respectively. Two consecutive processes of heating and cooling have been analyzed, and no relevant hysteretic phenomena have been observed.

## V. CONCLUSION

In this paper, a new hybrid telemetric MEMS has been proposed. The novel passive wireless sensor is capable of operating in harsh environments for high-temperature measurements. It consists of only passive elements: a planar inductor bonded to a microfabricated and temperature-sensitive variable capacitor. The hybrid sensor behaves as an  $LC$  resonant circuit, in which the variable capacitor represents the capacitance, and the planar inductor is the inductance. The telemetric system consisting of a readout inductor positioned a few centimeters outside the harsh environment and coupled with the hybrid MEMS has been characterized. The two inductors constitute a coupled transformer with the readout inductor connected to the measurement electronics and the planar inductor to the variable capacitor that is designed for high-temperature environments. Two different measurement techniques have been used. An experimental setup has successfully been designed to test the hybrid sensor at high temperatures. The whole system has been characterized in the laboratory, and several results were reported for temperatures up to  $330\text{ }^{\circ}\text{C}$ . The values measured by the two techniques have demonstrated good agreement with the reference values during both heating and cooling processes. In conclusion, the proposed telemetric system exploits the possibility to measure the temperature inside harsh and hermetic environments, and several experimental results show good agreement. Furthermore, one of the proposed techniques can be used in applications where it is necessary to compensate for changes in readout distance.

## ACKNOWLEDGMENT

The authors would like to thank the staff guided by Prof. Baglio of the University of Catania, for the support and the technical design of the MEMS.

## REFERENCES

- [1] M. V. P. Kruger, M. H. Guddal, R. Belikov, A. Bhatnagar, O. Solgaard, C. Spanos, and K. Poolla, "Low power wireless readout of autonomous sensor wafer using MEMS grating light modulator," in *Proc. IEEE/LEOS Int. Conf. Opt. MEMS*, 2000, pp. 67–68.
- [2] J. Rodríguez, J. Meca, J. A. Jimenez, and E. J. Bueno, "Monitoring and quality improvement of pharmaceutical glass container's manufacturing process," *IEEE Trans. Instrum. Meas.*, vol. 57, no. 3, pp. 584–590, Mar. 2008.
- [3] Z. D. Schwartz, A. N. Downey, S. A. Alterovitz, and G. E. Ponchak, "High-temperature RF probe station for device characterization through  $500\text{ }^{\circ}\text{C}$  and  $50\text{ GHz}$ ," *IEEE Trans. Instrum. Meas.*, vol. 54, no. 1, pp. 369–376, Feb. 2005.
- [4] C. Beaucamp-Ricard, L. Dubois, S. Vaucher, P. Y. Cresson, T. Lasri, and J. Pribetich, "Temperature measurement by microwave radiometry: Application to microwave sintering," *IEEE Trans. Instrum. Meas.*, vol. 58, no. 5, pp. 1712–1719, May 2009.

- [5] D. Mavrudieva, J. Y. Voyant, A. Kedous-Lebouc, and J. P. Yonnet, "Magnetic structures for contactless temperature sensor," *Sens. Actuators A, Phys.*, vol. 142, no. 2, pp. 464–467, Apr. 2008.
- [6] S. F. Lord, S. L. Firebaugh, and A. N. Smith, "Remote measurement of temperature in the presence of a strong magnetic field," *IEEE Trans. Instrum. Meas.*, vol. 58, no. 3, pp. 674–680, Mar. 2009.
- [7] M. A. Fonseca, J. M. English, M. Von Arx, and M. G. Allen, "Wireless micro-machined ceramic pressure sensor for high temperature applications," *J. Microelectromech. Syst.*, vol. 11, no. 4, pp. 337–343, Aug. 2002.
- [8] M. A. Fonseca, M. G. Allen, J. Kroh, and J. White, "Flexible wireless passive pressure sensors for biomedical applications," in *Proc. Tech. Dig. Solid State Sensor, Actuator, Microsyst. Workshop*, Hilton Head Island, SC, Jun. 2006, pp. 37–42.
- [9] Y. Jia, K. Sun, F. J. Agosto, and M. T. Quinones, "Design and characterization of a passive wireless strain sensor," *Meas. Sci. Technol.*, vol. 17, no. 11, pp. 2869–2876, Nov. 2006.
- [10] O. Akar, T. Akin, and K. Najafi, "A wireless batch sealed absolute capacitive pressure sensor," *Sens. Actuators A, Phys.*, vol. 95, no. 1, pp. 29–38, Dec. 2001.
- [11] E. D. Birdsell and M. G. Allen, "Wireless chemical sensors for high temperature environments," in *Proc. Solid-State Sens., Actuators, Microsyst. Workshop*, Hilton Head Island, SC, Jun. 4–8, 2006, pp. 212–215.
- [12] T. J. Harpster, B. Stark, and K. Najafi, "A passive wireless integrated humidity sensor," *Sens. Actuators A, Phys.*, vol. 95, no. 2/3, pp. 100–107, Jan. 2002.
- [13] E. Birdsell and M.G. Allen, "Wireless chemical sensors for high temperature environments," in *Proc. Tech. Dig. Solid-State Sensor, Actuator, Microsyst. Workshop*, Hilton Head Island, SC, Jun. 2006, pp. 212–215.
- [14] E. L. Tan, W. N. Ng, R. Shao, B. D. Pereles, and K. G. Ong, "A wireless, passive sensor for quantifying packaged food quality," *Sensors*, vol. 7, no. 9, pp. 1747–1756, 2007.
- [15] Y. Wang, Y. Jia, Q. Chen, and Y. Wang, "A passive wireless temperature sensor for harsh environment applications," *Sensors*, vol. 8, no. 12, pp. 7982–7995, 2008.
- [16] D. Marioli, E. Sardini, M. Serpelloni, B. Andò, S. Baglio, N. Savalli, and C. Trigona, "Hybrid telemetric MEMS for high temperature measurements into harsh industrial environments," in *Proc. I2MTC*, Singapore, 2009, pp. 1423–1428.
- [17] M. Suster, D. J. Young, and W. H. Ko, "Micro-power wireless transmitter for high-temperature MEMS sensing and communication applications," in *Proc. 15th IEEE Int. Conf. Micro Electro Mech. Syst.*, 2002, pp. 641–644.
- [18] L. H. Han and S. Chen, "Wireless bimorph micro-actuators by pulsed laser heating," *Sens. Actuators A, Phys.*, vol. 121, no. 1, pp. 35–43, May 2005.
- [19] B. Andò, S. Baglio, N. Pitrone, N. Savalli, and C. Trigona, "Bent beam MEMS temperature sensors for contactless measurements in harsh environments," in *Proc. IEEE I2MTC*, Victoria, BC, Canada, 2008, pp. 1930–1934.
- [20] D. Marioli, E. Sardini, and M. Serpelloni, "An inductive telemetric measurement system for humidity sensing," *Meas. Sci. Technol.*, vol. 19, no. 11, pp. 115204-1–115204-8, Nov. 2008.



**Daniele Marioli** (M'04) was born in Brescia, Italy, on January 21, 1946. He received the Laurea degree in electrical engineering from the University of Pavia, Pavia, Italy, in 1969.

Since 1969, he has been involved in research and educational activities with Politecnico di Milano, Milan, Italy, and the University of Brescia, Brescia, where he has been a Full Professor of electronics since 1990 and Chief of the Department of Electronics for Automation, Faculty of Engineering. The activities in these fields are related to the realization of

innovative sensors in thick-film technology based on piezoelectric, pyroelectric, and piezoresistive behaviors of screen-printable pastes, and in microelectromechanical systems technology for the detection of physical quantities (acceleration, force, pressure, mass, etc.); the realization of high-resolution electronic instrumentation for capacitive measurements; the design and realization of integrated electronic circuits as the front-end of piezoresistive-based sensors; the development of new linearization techniques based on neural networks; and the development of web sensors and wireless sensors. He is the author or coauthor of more than 200 scientific papers published in international and national journals and conference proceedings and is the holder of four patents. His research interests include the design, realization, and test of sensors, electronic instrumentation, and signal processing electronic circuits.



**Emilio Sardini** (M'04) was born in Commessaggio, Mantova, Italy, in 1958. He received the Laurea degree in electronic engineering from Politecnico di Milano, Milan, Italy, in 1983.

Since 1984, he has been with the Department of Electronics for Automation, Faculty of Engineering, University of Brescia, Brescia, Italy, where he was an Assistant Professor from 1986 to 1998, an Associate Professor of electrical and electronics measurements in 1998, and is currently a Full Professor. He teaches courses in electronics instrumentation. His research

activity has been on sensors and electronic instrumentation, particularly the conditioning electronics of capacitive and inductive sensors, microprocessor-based instrumentation, the development of thick-film sensors, and instrumentation for noise, as well as low-frequency acceleration measurements.



**Mauro Serpelloni** was born in Brescia, Italy, in 1979. He received the Laurea degree (*summa cum laude*) in industrial management engineering and the Research Doctorate degree in electronic instrumentation from the University of Brescia, Brescia, in 2003 and 2007, respectively.

He is currently a Research Assistant of electrical and electronic measurements with the Department of Electronics for Automation, Faculty of Engineering, University of Brescia. He has worked on several projects relating to the design, modeling, and fabrication

of measurement systems for industrial applications. His research interests include contactless transmissions between sensors and electronics, contactless activation for resonant sensors, and signal processing for microelectromechanical systems.